JOURNAL OF VIROLOGY, Oct. 1977, p. 673-684

Vol. 24, No. 2
Printed in U.S.A.

Electron Microscopic Studies of Bacteriophage M13 DNA Replication

D. P. ALLISON,* A. T. GANESAN,† A. C. OLSON, C. M. SNYDER, AND S. MITRA

Biology Division, Oak Ridge National Laboratory, Oak Ridge, Tennessee 37830

Received for publication 13 June 1977

Intracellular forms of M13 phage DNA isolated after infection of *Escherichia coli* with wild-type phage have been studied by electron microscopy and ultracentrifugation. The data indicate the involvement of rolling-circle intermediates in single-stranded DNA synthesis. In addition to single-stranded, circular DNA, we observed covalently closed and nicked replicative-form (RF) DNAs, dimer RF DNAs, concatenated RF DNAs, RF DNAs with single-stranded tails (σ, rolling circles), and, occasionally, RF DNAs with θ structures. The tails in σ molecules are always single stranded and are never longer than the DNA from mature phage; the proportion of σ to other RF molecules does not change significantly with time after infection. The origin of single-stranded DNA synthesis has been mapped by electron microscopy at a unique location on RF DNA by use of partial denaturation mapping and restriction endonuclease digestion. This location is between gene IV and gene II, and synthesis proceeds in a counterclockwise direction on the conventional genetic map.

M13 phage belongs to the group of filamentous phage specific for male strains of *Escherichia coli* and contains circular, single-stranded DNA (ssDNA) with a mass of 2×10^6 daltons (26). Pratt and Erdahl (23) showed that there are three basic stages of M13 DNA replication after infection. These are analogous to those of ϕX174, namely, (i) replication of parental ssDNA to parental replicative-form (RF) DNA; (ii) synthesis of progeny RF DNA; and (iii) synthesis of progeny ssDNA from RF DNA. Stage i does not require any phage-induced proteins; stage ii requires M13 gene 2 protein; and stage iii requires both gene 2 and 5 proteins (23). The gene 5 product, a small ssDNA-binding protein, is essential for progeny ssDNA synthesis (19). After infection with M13 gene 5 amber mutant (*am5*) phage, progeny ssDNA synthesis is absent. Dressler (6) showed that ϕX174 ssDNA synthesis occurs by the rolling-circle (σ) model (10); Ray (25) showed by ultracentrifugal analysis of pulse-labeled intracellular M13 DNA that the virus strand is continuously displaced from the RF DNA and chased into progeny ssDNA. Our examination of intracellular M13 DNA by electron microscopy and ultracentrifugation indicated that ssDNA synthesis occurs by a σ mechanism. This report includes a partial denaturation map of the σ intermediates that shows a unique origin of ssDNA synthesis. The correlation of the partial denaturation map and the genetic map establishes that the origin of M13 ssDNA synthesis is in or near gene II and that there is a counterclockwise direction of replication in reference to the genetic map. During the preparation of this manuscript, Horiuchi and Zinder (12) and Suggs and Ray (31) independently showed the unique origin and direction of progeny ssDNA synthesis. Our data agree with theirs. A preliminary report of this work has been published (D. P. Allison, A. T. Ganesan, and S. Mitra, Fed. Proc. **33**:1491, 1974).

† Permanent address: Department of Genetics, Stanford University Medical School, Stanford, CA 94305.

MATERIALS AND METHODS

Bacteria and phage. *E. coli* K37 (from D. Pratt) was used as the wild-type host. Isogenic *E. coli* K38 (*su*$^-$), obtained from P. Model, was used as the nonpermissive host. Wild-type M13 phage and M13 *am5*, obtained from D. Pratt, were further purified from single-plaque isolates. The mutant phage stock had less than 0.1% revertants.

Growth media and buffers. The growth and purification of phage and the extraction and purification of phage DNA have been described (20). The following buffers were used routinely: buffer A, 0.1 M NaCl, 0.05 M Tris-hydrochloride (pH 8.0), and 0.001 M EDTA; buffer B, 1 M NaCl, 0.02 M Tris-hydrochloride (pH 8.0), and 0.002 M EDTA; buffer C, 0.01 M Tris-hydrochloride (pH 8.0) and 0.001 M EDTA.

Chemicals and enzymes. Pronase (B grade), pancreatic RNase, cytochrome *c*, and ethidium bromide were purchased from Calbiochem, La Jolla, Calif. Before use, Pronase solution (10 mg/ml) in buffer A was self-digested at 37°C for 30 min, and RNase was heated at 100°C for 10 min. The [*methyl*-^{3}H]thymidine (6 to 20 Ci/mmol) was purchased from Amer-

sham/Searle, Arlington Heights, Ill., or New England Nuclear Corp., Boston, Mass., and carrier-free $H_3{}^{32}PO_4$ was obtained from Amersham/Searle. Sarkosyl NL97 was a gift of Ciba-Geigy, and sodium dodecyl sulfate was a BDH Chemicals product. All other chemicals were of reagent grade.

The purification and digestion with *E. coli* exonuclease I and *Haemophilus influenzae* restriction endonuclease (*Hin*dII) have been reported earlier (4). *H. aegypticus* restriction endonuclease (*Hae*II) was a gift of R. diLauro of the Public Health Service, National Cancer Institute, Bethesda, Md. This enzyme was used according to the method of van den Hondel and Schoenmakers (35).

Isolation of intracellular phage DNA. *E. coli* cultures grown to log phase (2×10^8 to 4×10^8 cells/per ml) in supplemented M9 medium (23) at 37°C were infected (multiplicity of infection, 100 to 200) with wild-type M13 and maintained at 37°C or infected with M13 *am*5 and maintained at 34°C, unless otherwise stated. The cultures were labeled with 20 μCi of [^{3}H]dThd per ml 8 or 45 min postinfection and, after specified times, were dumped into equal volumes of chilled poison to stop bacterial synthesis. The poison was either buffer A containing KCN (10^{-2} M) and pyridine (5%) (15) or 75% ethanol, 21 mM sodium acetate (pH 5.3), 2 mM EDTA, and 2% phenol (22). The cells were then harvested by low-speed centrifugation and washed twice with buffer A containing 10^{-2} M KCN. Sometimes the cell suspensions were shaken in a VirTis homogenizer for 2 min at low setting to remove unadsorbed phage particles.

Next, the cells were suspended in 1/10 to 1/20 volume of buffer A and incubated in the presence of lysozyme (200 μg/ml) at 0°C for 45 min (25). The cells were then lysed with Sarkosyl NL 97 (0.5%) for 15 min at 37°C and digested with Pronase (200 μg/ml) at 37°C for 30 to 60 min. In some experiments lysis was accomplished by adding sodium dodecyl sulfate (0.8%) to cells suspended in 50 mM Tris-hydrochloride (pH 8.0) containing 5 mM EDTA in 10% sucrose (11). Finally, the lysates were gently layered on top of 20% sucrose in buffer B in an SW27 swinging-bucket rotor tube and centrifuged at 25,000 rpm for 3 to 4 h at 15°C in a Beckman-Spinco ultracentrifuge. The liquid was taken from the top without disturbing the bacterial DNA, which sedimented at or near the bottom of the tube. After phenol extraction in the presence of 1% sodium dodecyl sulfate and subsequent alcohol precipitation, the phage DNA was dissolved in buffer C. Occasionally, the DNA samples were treated with RNase (50 μg/ml, 37°C, 1 h) before electron microscopy.

Ultracentrifugal analysis. Equilibrium ultracentrifugation in CsCl containing ethidium bromide (1) (4.2 g of CsCl and 0.4 ml of 5-mg/ml ethidium bromide per 4.0 ml of DNA) was carried out in polyallomer tubes in a no. 40 rotor of a Beckman-Spinco ultracentrifuge. After 40 to 50 h of centrifugation at 35,000 rpm and 23°C, 30 to 40 fractions were collected from the bottom, and portions were assayed for radioactivity. Ethidium bromide from the pooled fractions was removed by repeated extraction with isopropanol (saturated with 30% [wt/wt] CsCl in 0.2 M Tris-hydrochloride [pH 8.0]) followed by dialysis against buffer C. For equilibrium ultracentrifugation in alkaline CsCl (8), 7.65 g of CsCl was added to 5.5 ml of DNA solution in 40 mM K_2PO_4 (pH 12.1) and centrifuged in a Beckman no. 40 rotor at 35,000 rpm for 42 h at 23°C.

Band sedimentation in neutral sucrose (5 to 20% sucrose in buffer B) and alkaline sucrose (5 to 20% sucrose in 0.8 M NaCl, 0.2 M NaOH, and 2 mM EDTA) gradients was accomplished in a Beckman SW41 swinging-bucket rotor. To trap the fast-moving, covalently closed, supercoiled RF type I (RFI) DNA, we sometimes used a 0.5-ml cushion of 60% CsCl and 60% sucrose (wt/wt) at the bottom.

Radioactivity measurement. The portions were either counted directly in aqueous medium in a Triton X-100–toluene scintillation solvent system or spotted on Whatman 3 MM disks and washed with 5% trichloroacetic acid, alcohol, and ether, in succession, to remove acid-soluble radioactivity. The dried disks were counted in toluene containing 2,5-bis[2-(5-*ter*-butylbenzoxazolyl)]thiophene (BBOT) (20).

Electron microscopy. Samples of DNA were prepared for electron microscopy by the Inman and Schnös (13) modification of the protein film technique (16). Fractions from sucrose or CsCl gradients were dialyzed against buffer C for 3 h at room temperature. A 0.07-ml sample was mixed with 0.03 ml of buffer (4 ml of 37% formaldehyde, 0.32 ml of 1 M Na_2CO_3, and 0.4 ml of 0.126 M EDTA) adjusted before mixing to either pH 8.7 (neutral) or 11.1 (denatured) with 1 N HCl or 5 N NaOH, respectively. After incubating for 10 min at 25°C, the DNA-buffer solutions were transferred to an ice bath, cooled for 5 min, and mixed with an equal volume of formamide (Mallinckrodt, 99%). Cytochrome *c* was then added to 0.01%, and the solutions were incubated for 10 min at room temperature before spreading 0.005 ml onto the surface of a water droplet. The DNA was picked up on nitrocellulose films supported on 400-mesh grids, rinsed in 95% ethanol, stained with uranyl acetate (5), rinsed in isopentane, and rotary shadowed with platinum at a 6° angle. Electron micrographs were taken on a Siemens Elmiskop 1A, with magnifications calibrated by using a diffraction grating replica (Fullam, 54,864 lines per inch). The micrographs were projected onto paper and traced, and the tracings were measured with a curvimeter to the nearest 0.05 μm. Under our conditions, there was no statistically significant difference in the contour lengths of M13 circular ssDNA and RFI DNA; therefore, it was not necessary to use a correction factor to correlate measurements of ssDNA and double-stranded DNA.

Alignment of partially denatured rolling circles. The partially denatured circles were aligned for maximum overlap of denatured regions by a correlation method similar to, but computationally simpler than, that of Young et al. (36). Computations were carried out on a PDP11/40 computer. Each molecule was divided into 100 segments; each segment was assigned a value of zero if the segment was more than half native, or of one if it was more than half denatured. A molecule was aligned to another by shifting one relative to the other a segment at a time, flipping it, and again shifting. The measure of overlap for each relative alignment was

$$\sum_{i=1} (X_i + Y_i)^2$$

where X_i and Y_i are the values assigned to the ith segment of each of the two molecules. Before the alignment, the molecules were ordered by their extent of denaturation, from most to least. The alignment procedure considered the molecules in that order, aligning the second to overlap maximally with the first. The third was then aligned to the sum of the first two, the fourth to the sum of the first three, etc. When all of the molecules had been aligned in this way, a second cycle, for refinement, was performed. In this cycle, each molecule was considered in the same order as before. Its contribution was subtracted from the sum; the molecule was aligned with the sum of the remaining molecules and added back to the sum in this new position. The differences between the results of the first and second cycles were quite minor. The resulting alignment was then translated to bring it into correspondence with the picture of partially denatured *Hin*d-cut, linear M13 RF DNA molecules.

RESULTS

Intracellular forms of M13 DNA. The M13 DNA isolated from cells 8 min after infection with wild-type phage was spread directly for electron microscopy or subjected to equilibrium centrifugation in CsCl containing ethidium bromide to separate covalently closed DNA (heavy band) from the rest (light band) (Fig. 1). Portions from the heavy and light bands were freed of dye, dialyzed, and then subjected to electron microscopy. The different intracellular forms of M13 DNA found in the heavy and light bands are shown in Fig. 2 and 3, respectively. The structures in the heavy band from DNA isolated 8 min postinfection include unit-length (2 μm) supercoiled RFI (Fig. 2A), dimer-length supercoiled RF (<1%) (Fig. 2B), and RF concatenates (ca. 5%) (Fig. 2C). We have previously shown that when RFI DNA is spread with formamide-formaldehyde, it contains a small, denatured region as depicted in Fig. 2A (S. Dasgupta et al., J. Biol. Chem., in press) and does not appear supercoiled. It has been postulated that the dimers and concatenates arise from errors in segregation of daughter molecules after one round of replication (9). We have found very few (2/≃1,000) M13 molecules with a θ structure like those found in the replicating intermediates of *E. coli* (3) or colicin E1 (14) DNA. The molecule shown in Fig. 2D is a circle with two forks that is 2 μm when only one branch of the double-stranded fork is included in the measurement. It appears possible that such structures, also observed by Ray (26), are intermediates in RF DNA replication.

The light band from the CsCl gradient portrayed in Fig. 1 contains 70 to 80% RF type II (RFII) DNA molecules (relaxed RF DNA with one or more discontinuities in one or both strands) (Fig. 3A), ssDNA circles (Fig. 3B), and σ structures with an ssDNA tail attached to RF

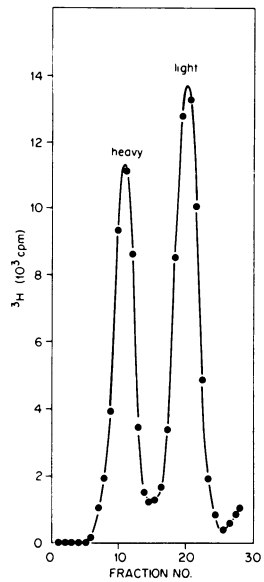

FIG. 1. *Equilibrium centrifugation of intracellular M13 DNA in CsCl containing ethidium bromide. A 100-ml log-phase culture of E. coli K37 grown in supplemented M9 medium at 37°C was infected with wild-type M13 for 8 min and then labeled with [^{3}H]-dThd for 90 s. After isolation of the total phage DNA, it was subjected to equilibrium centrifugation in CsCl containing ethidium bromide (both procedures as described in the text). Fractions were collected from the bottom and monitored for radioactivity. Sedimentation was from right to left. The density of the heavy band was 1.60 g/ml and that of the light band was 1.56 g/ml.*

DNA (Fig. 3C). The tailed molecules are expected intermediates for ssDNA synthesis on circular, double-stranded DNA templates (10), and the tails generally appear distinctly single stranded in our electron micrographs. Dressler (6) observed similar structures during φX174 DNA synthesis, and Ray (26) also detected such molecules in intracellular M13 DNA. Because we never, in examining more than 200 σ molecules, found tails longer than 2 μm (unit length), we conclude that the single strands of the rolling circle are cleaved as soon as they reach mature virus DNA length. Figure 3D shows a molecule with two single-stranded tails attached to RF DNA; about 10% of the tailed molecules had two tails.

Figure 4 shows a σ molecule spread at pH 11.1 in the presence of 50% formamide, conditions under which the double-stranded DNA is partially denatured. That the frequency of such σ structures did not decrease under this condition demonstrates that the ssDNA tails are indeed covalently attached to the double-stranded RF DNA molecules, and the absence of any

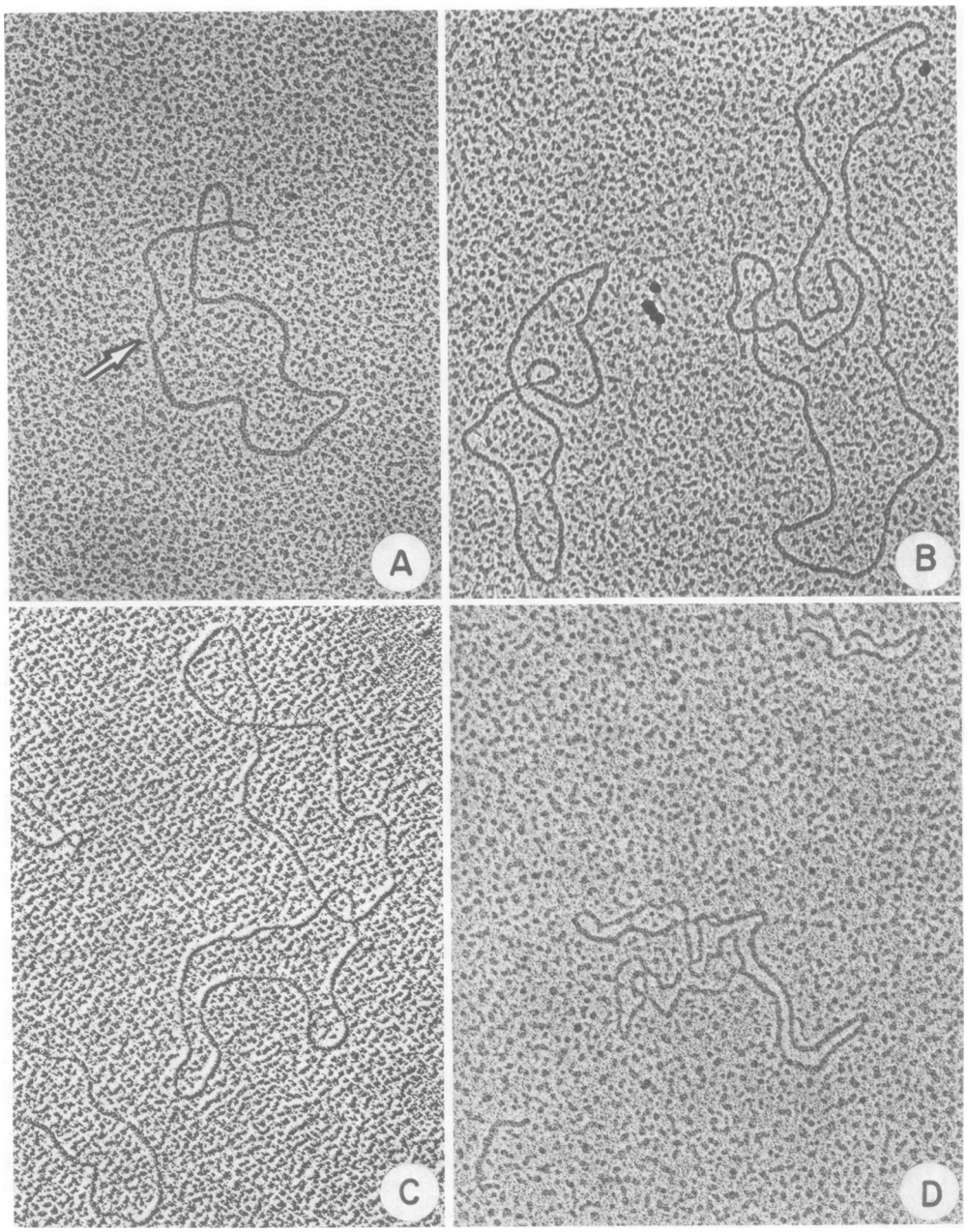

FIG. 2. *Forms of intracellular M13 DNA in the heavy band represented in Fig. 1. Supercoiled RFI molecules (A) appear open when spread with formamide. The small denatured area (arrow) is nearly always present when supercoiled molecules are spread under these conditions. Dimer-length, supercoiled RF (B), concatenates (C), and a few θ structures (D) are also present.* ×57,560.

denatured areas in the tails is a clear indication of their single strandedness. No double-stranded tails were seen among a few hundred σ structures subjected to denaturation. This suggests that RF replication of M13 DNA does not occur via a double-stranded σ intermediate, and is, in this respect, different from that of φX174 (28).

After *E. coli* infection by wild-type M13, RF replication predominates for the first 10 to 20 min, after which progeny ssDNA is the major

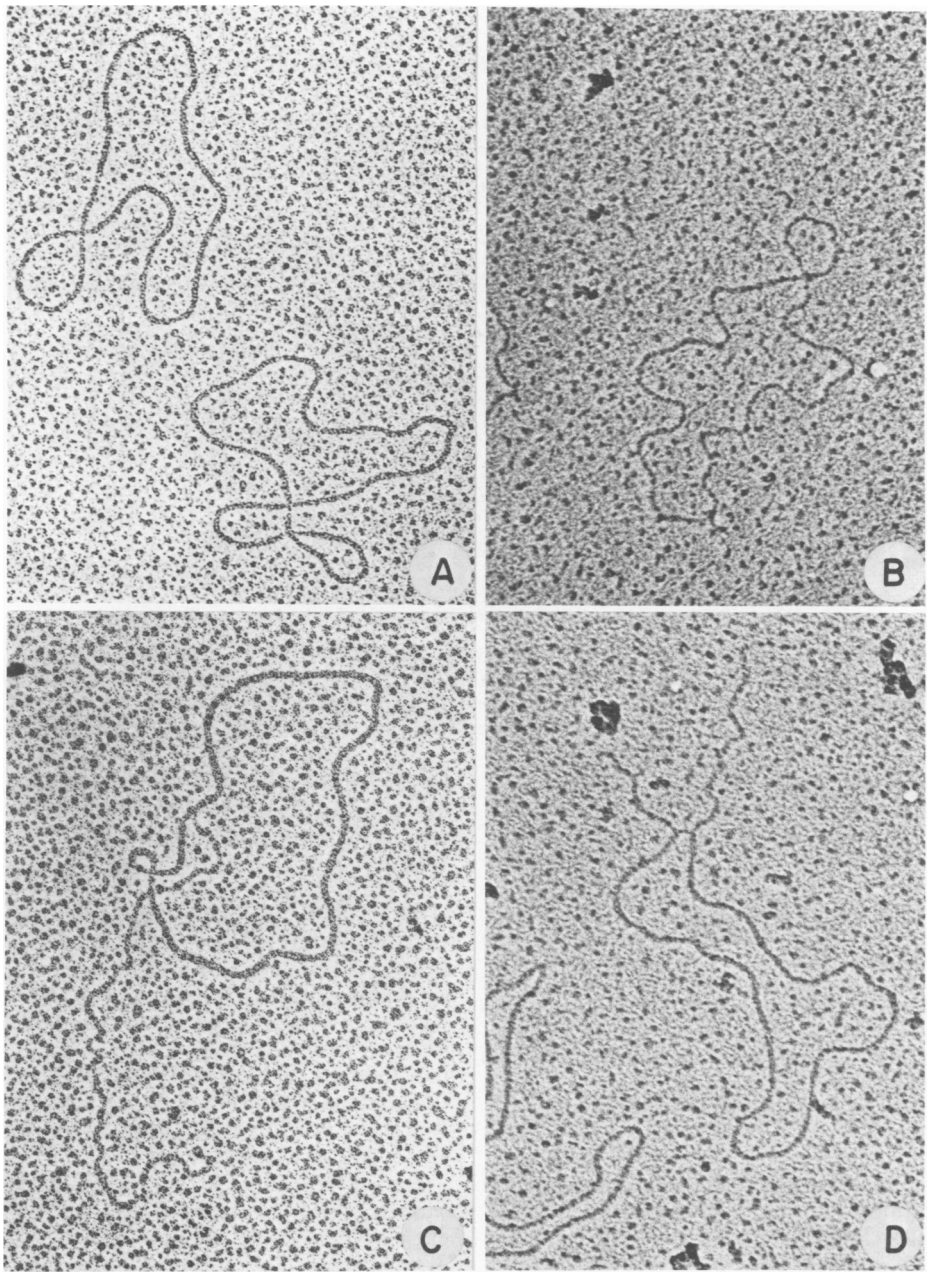

FIG. 3. *Forms of intracellular M13 DNA in the light band represented in Fig. 1. (A) Relaxed RFII circles that never exhibit the small denatured area found in the supercoiled circles. Unit-length, single-stranded circles (B) are also present, as well as circular RF molecules with single-stranded linear tails (σ). Most of these molecules exhibit a single-stranded tail attached to a double-stranded circle (C). However, some molecules are found with two single-stranded tails issuing from the RF molecule (D).* ×57,560

form synthesized (26). However, we saw tailed molecules as early as 8 min after wild-type infection (Fig. 3), and the frequency of these tailed molecules in the total RF DNA population appeared to be independent of the time after infection (Table 1). We therefore agree with Forsheit et al. (7), who showed that some progeny ssDNA synthesis occurs very early after infection.

We found no tailed molecules in DNA extracted from *E. coli* K38 10 to 15 min after

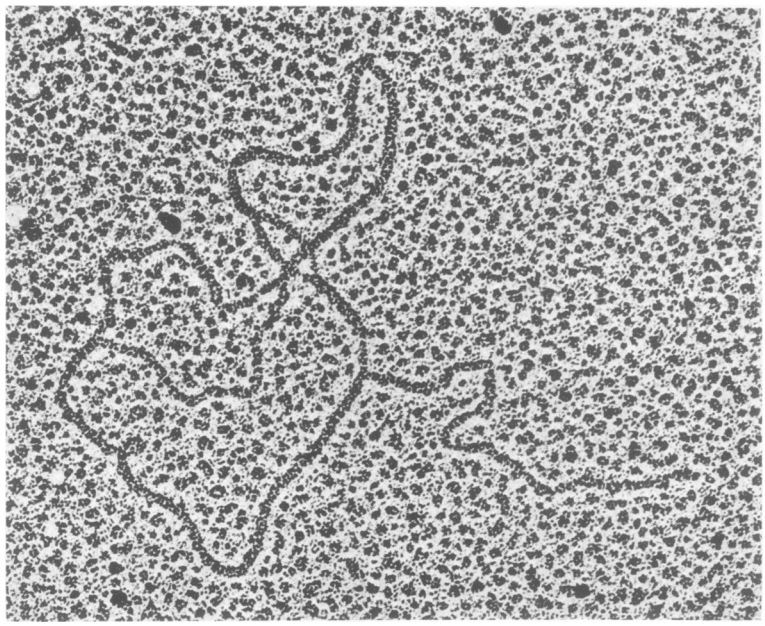

FIG. 4. *Partially denatured RF DNA with tail. DNA isolated from the light band represented in Fig. 1 was adjusted to pH 11.1 for 10 min before spreading for electron microscopy. Two denatured sites are evident on the circular RF molecule. The single-strandedness of the tail can be inferred because the tail does not contain any denatured sites and appears less thick than the RF molecule. ×110,000.*

TABLE 1. *Percentage of RF molecules with single-stranded tails early and late postinfection*[a]

Expt	Early	Late
1	37/237 (16)[b]	47/247 (19)
2	4/38 (11)	5/41 (12)

[a] Log-phase *E. coli* cultures (100 ml) were infected with wild-type M13 phage (multiplicity of infection, ~100). Total intracellular DNA, after removal of the host DNA as described in the text, was spread for electron microscopy after RNase treatment and deproteinization. "Early" and "late" refer to 8 and 45 min postinfection at 37°C.

[b] Number in parentheses represents percent.

infection with M13 *am5* phage in three separate preparations, scoring approximately 500 RF molecules. The presence of M13 gene 5 protein, therefore, appears to be essential for the existence of the σ structure.

Ultracentrifugal studies of M13 ssDNA synthesis. Ultracentrifugal analysis and detection of longer-than-unit-length, pulse-labeled DNA of virus-strand type led Ray (25) and Tseng and Marvin (33) to propose that M13 ssDNA synthesis occurs by a rolling-circle mechanism. To complement our electron microscopic evidence for the involvement of σ structures in M13 ssDNA synthesis (to be presented later), we extended the earlier ultracentrifugal studies by investigating DNA from both wild-type and *am5* phages. Band sedimentation analyses in neutral sucrose of both pulse-labeled M13 wild type and *am5* DNA early and late postinfection showed that most of the label was present in RFI and RFII, with very little or no incorporation into mature ssDNA, in agreement with Ray (25) (data not shown). After infection with wild-type phage, a large fraction (70 to 80%) of this label can, however, be transferred to ssDNA after a chase (4, 25). In contrast, in M13 *am5*-infected cells, in the absence of ssDNA synthesis, the effect of a similar pulse and chase was only to transfer label from RFII to RFI (S. Dasgupta and S. Mitra, in preparation).

A more revealing set of experimental results was obtained from extended band sedimentation of pulse-labeled DNAs in alkaline sucrose (Fig. 5) where RFI DNA sediments into the cushion at the bottom while RFII DNA separates into unit-length linear single strands, circular single strands, and longer-than-unit-length single strands. It is evident by comparing with the marker phage DNA that in both early (A) and late (B) postinfection with wild-type phage, the label is distributed bimodally into unit-length linear DNA (16S) and a faster-sedimenting DNA with a sedimentation coefficient of ca. 20S. The faster-sedimenting DNA did not correspond exactly with, but contained material that moved

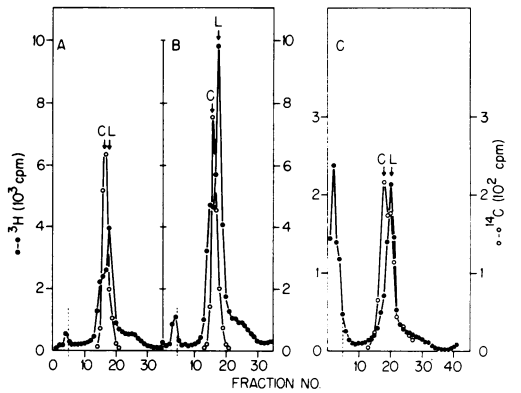

FIG. 5. *Band sedimentation in alkaline sucrose of pulse-labeled wild-type and am5 M13 DNA. Twenty-milliliter log-phase cultures of E. coli K37 (A and B) and K38 (C) infected with wild type (A and B) and am5 phage (C) were pulse-labeled with 20 μCi of [^{3}H]thymidine per ml as described in the text. (A) 30-s pulse-label at 37°C, 8 min postinfection; (B) 30-s pulse-label at 37°C, 45 min postinfection; (C) 1-min pulse-label at 25°C, 3 min after shift-down to 25°C from 37°C, 13 min postinfection. After termination of labeling, the infected cells were washed and lysed, and the bacterial DNA was removed by centrifugation as described in the text. Portions of the DNA, along with ^{14}C-labeled M13 phage DNA, were centrifuged in 5 to 20% alkaline sucrose gradients in a Beckman SW41 swinging-bucket rotor at 5°C at 39,000 rpm for 11 h (A, B) or 38,000 rpm for 12 h (C). Symbols: ●, ^{3}H; ○, ^{14}C. The positions of circular and unit-length, linear M13 DNA are indicated by C and L, respectively. RFI DNA sedimenting into the cushion is indicated by a dashed line.*

faster than, the circular phage DNA. In contrast, DNA extracted from M13 *am5*-infected culture (C) early postinfection sedimented mainly as unit-length linear DNA in alkaline sucrose, with little labeled material sedimenting faster than circular DNA. A significant amount of label is also in the RFI DNA. Figure 6 shows that following the chase of pulse-labeled DNA after wild-type M13 infection, the label from both unit-length linear DNA and the faster-moving DNA (20S peak) is in the DNA that sediments exactly with circular DNA marker.

These results can easily be explained by the situation depicted in our electron micrographs, where longer-than-unit-length strands (i.e., circles with tails) are clearly evident. If these are indeed intermediates in ssDNA synthesis, any label they contain should be chased into mature circular DNA during continued synthesis with unlabeled thymidine. This proposition was tested in two ways: First, the pulse-labeled fractions containing longer-than-unit-length linear DNA (Fig. 6A) and the corresponding chased fractions (Fig. 6B) were separately pooled. The DNAs were then tested for susceptibility to *E. coli* exonuclease I, which attacks only ssDNA from the 3′ end. Circular phage DNA is completely resistant to this exonuclease (20). The majority of the label from pulse-labeled DNA is susceptible to the exonuclease (Table 2), indicating that most of the DNA sedimenting in the position of circular DNA is, in fact, longer-than-unit-length linear DNA. The majority of the DNA isolated after chasing is, as expected, resistant to the exonuclease and, therefore, cir-

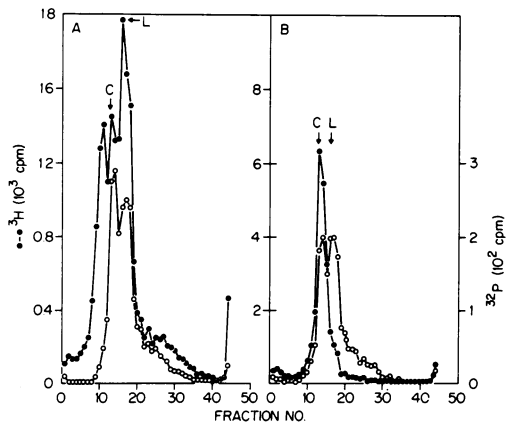

FIG. 6. *Band sedimentation in alkaline sucrose of wild-type M13 DNA after pulse and chase. E. coli K38 infected with phage was labeled with [^{3}H]dThd for 30 s 45 min postinfection at 37°C. One half of the culture (A) was stopped with ethanol-phenol mix (22), while the other (B) was treated with 500 μg of unlabeled dThd per ml for 10 min before addition of the stopper. Further processing and centrifugation are described in the legend to Fig. 5C, except M13 virion [^{32}P]DNA was used as the internal marker.*

TABLE 2. *Susceptibility of alkali-denatured, pulse-labeled M13 DNA to exonuclease I*[a]

Type of DNA	DNA made acid soluble by exonuclease I (%)	
	[^{3}H]DNA	Control [^{32}P]-DNA
After pulse-labeling (Fig. 7A)	74.4	91.2
After chase (Fig. 7B)	35.6	89.8

[a] The fractions 8 to 19 and 10 to 17 in Fig. 6A and B, respectively, were pooled, quickly neutralized, and alcohol precipitated in the presence of 0.3 M sodium acetate. Portions (~4 × 10^3 cpm) of the dissolved precipitate were mixed with 75 pmol of pancreatic DNase-treated and denatured ^{32}P-labeled M13 RF DNA (4.7 × 10^3 cpm) (G. Lavelle and S. Mitra, *in* P. Tattersall and D. Ward, ed., *Parvoviruses*, in press) and then digested with 0.6 U of *E. coli* exonuclease I in 0.3 ml at 37°C for 30 min (20).

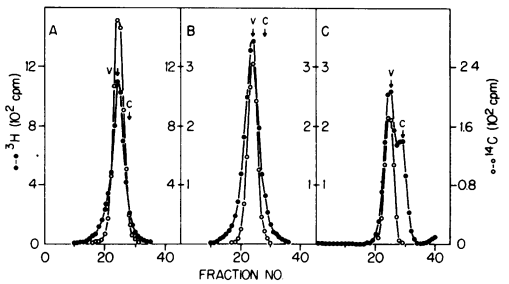

FIG. 7. *Equilibrium centrifugation in alkaline CsCl. Pooled fractions of unit-length, linear and longer-than-unit-length M13 DNA pooled from the alkaline sucrose gradient of Fig. 5 were banded in alkaline CsCl as described in the text. (A) Longer-than-unit-length ssDNA from fractions 13 to 16 of Fig. 5B; (B) unit-length, linear ssDNA from fractions 17 to 20 of Fig. 5B; and (C) unit-length, linear ssDNA from fractions 18 to 22 of Fig. 5C. Symbols: ●, ^3H; ○, ^{14}C marker phage DNA. (v) and (c) denote the position of viral and complementary strands, respectively.*

cular. Second, equilibrium centrifugation in alkaline CsCl (Fig. 7) was used to determine the strandedness of (B) unit-length and (A) longer-than-unit-length linear DNA samples from pulse-labeled DNA late after wild-type phage infection (pooled from fractions in Fig. 5B) and of (C) pulse-labeled, unit-length linear DNA after M13 *am*5 infection (Fig. 5C). The pulse-labeled linear DNA from M13 *am*5-infected cells contained both viral and complementary strands in an equimolar amount after correcting for differences in thymine content (26), whereas the label in the DNA from wild-type M13-infected cells late postinfection contains predominantly viral strands, which is in agreement with the results of Suggs and Ray (31).

Origin of ssDNA synthesis on RF DNA template. All the experiments described so far indicate that progeny M13 ssDNA synthesis, like that of ϕX174 DNA, occurs by a σ mechanism where the 3′ end of the growing virus strand displaces the 5′ end of the same strand on the complementary strand template of RF DNA. If the synthesis starts at a fixed site on the RF template, it should be possible to locate the site by visually "folding" the single-stranded tail back on the circular part of the σ structure shown in electron micrographs. The basic problem of such a method lies in establishing a point of reference in the circular RF DNA, but we circumvented this difficulty by taking advantage of the site of cleavage by *Hin*dII restriction endonuclease on M13 RF (34). This enzyme does not attack M13 ssDNA (2). Total phage DNA was extracted from 100 ml of *E. coli* K37 culture in supplemented M9 medium, 45 min after infection with wild-type M13. After treatment of the DNA solution with *Hin*d endonuclease (4), the DNA was spread for electron microscopy in the presence of formamide at pH 8.7 as described in Materials and Methods. We were thus able to observe linear RF DNA (2 μm long) with or without single-stranded tails of various lengths attached to the double-stranded DNA. The length of the tail was measured in both directions from the three-point junction, giving two possible locations for the origin of ssDNA synthesis. Assuming there is a unique origin of synthesis, only one of the two sites from each molecule, in an array of different molecules, would be common to all. Because the "right" and "left" ends of the double-stranded RF DNA could not be distinguished, we could only establish the distance of the origin from the *Hin*d cleavage site. Figure 8 represents a collection of molecules with the two possible origins, one indicated for each molecule on either side of the three-point junction. It is quite clear that only one region, corresponding to about 0.2 μm from the *Hin*d cleavage site, is common to most of the molecules. The direction of replication can be established in a relative sense in

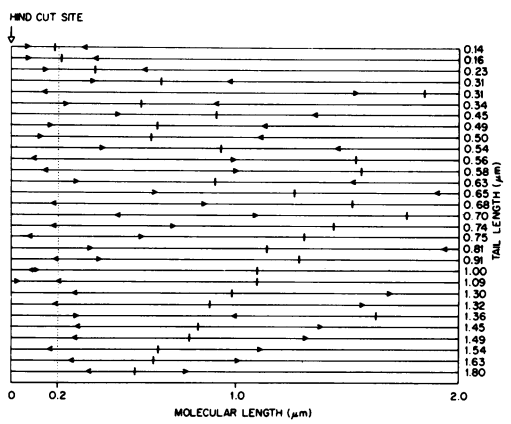

FIG. 8. *Mapping of single-stranded tails on linear RF DNA. The total viral DNA was purified from K37 cultures, maintained at 37°C, 45 min after infection with wild-type M13 as described in the text. After digestion of the DNA with Hind endonuclease, it was spread for electron microscopy as described in the text. The "Y"-shaped molecules arising from σ structures were photographed. The double-stranded arms were measured and normalized to 2 μm, and the length of the single-stranded tail was interpolated onto the double-stranded arms. The two possible origins of ssDNA synthesis thus obtained are indicated by arrows on the lines representing the RF DNA molecules. The molecules are oriented so that, of the two possible origins, the one closest to the Hind cut is located on the left. The numbers at the end of the lines indicate tail length.*

that the DNA chain grows either toward or away from the center of the double-stranded template. However, one problem that may complicate such a determination is branch migration occurring in vitro (17) after replicating DNA has been freed of gene 5 protein, which in vivo covers up the peeled-off 5′ end of the strand (24) and prevents branch migration. Branch migration in DNA would, in effect, apparently reverse the direction of synthesis. In fact, we can see both directions of chain growth in Fig. 8. However, we may assume that the possibility of branch migration is significantly reduced in molecules with longer single-stranded tails, and these molecules (shown in the lower half of the array) clearly indicate that the direction of chain growth is away from the center of the molecules.

To establish the absolute direction of chain growth and relate it to the genetic map of the phage, we utilized the partial denaturation mapping technique of Inman and Schnös (13). The partial denaturation map (Dasgupta et al., J. Biol. Chem., in press) of linear RF DNA generated by *Hin*d endonuclease cleavage was then related to the *Hae*II restriction endonuclease map (35) that had already been related to the genetic map of the phage (18). We utilized the fact that glyoxal predominantly fixes a region in supercoiled M13 RF DNA that corresponds to the major denaturable region and digested glyoxal-treated M13 RFI DNA with *Hae*II, which cuts the DNA into three pieces of 3,500, 2,600, and 320 base pairs, denoted as A, B, and C, respectively (35). A comparison of the *Hae*II restriction map and the partial denaturation map of *Hin*d endonuclease-generated linear DNA (Fig. 10) shows that the glyoxal-fixed bubble corresponding to the major A-T-rich region would be located in the B fragment if the orientation of the denaturation map were the same as that of the conventional restriction map (i.e., with the intragenic region located near the *Hin*d site in a clockwise direction [35] or on the right side of the *Hin*d site in a similarly oriented linear representation). Alternatively, the bubble would be in the A fragment if the molecules in the partially denatured map were oriented in the opposite way. Out of 43 DNA fragments scored, 12 contained bubbles, and 11 of these (>90%) fell in the size range corresponding to 2,300 to 2,500 base pairs. The bubble-containing fragments, therefore, clearly correspond to *Hae*II B fragments. This establishes the orientation of the partial denaturation map relative to the *Hae*II restriction map and, by extension, to the genetic map.

To establish the origin and direction of ssDNA synthesis, we partially denatured circular RFII molecules (Fig. 4) by raising the pH to 11.1 for 10 min before spreading for electron microscopy. Molecules with single-stranded tails were measured so that both the position and length of the denatured areas and the single-stranded tails could be related to a convenient, but arbitrary, starting point on the circular molecules. The data were fed into the computer, where the molecules were normalized to 2 μm and aligned for maximum overlap of denatured regions as described in Materials and Methods. We then asked the computer to translate these data to correspond to the partial denaturation profile of RFI molecules that had been cleaved by the site-specific *Hin*dII endonuclease before denaturation. The *Hin*dII-cut molecules represented in Fig. 9A are plotted so that the site of the predominant denatured area is in the left half of the moleules; the array of partially denatured RFII molecules with single-stranded tails arranged by the computer are represented in Fig. 9B. When the single-stranded tails of various lengths are superimposed onto these partially denatured RF molecules, they indicate a common origin of replication. If the best-fit data plotted by the computer are used, out of the 39 molecules shown, 31 have a common origin located 0.16 μm (standard deviation = 0.12 μm out of a total length of 2.0 μm) or about 8% from the left end of the map with the direction of chain growth away from the center. We should point out that eight molecules (indicated by dotted circles around the two possible origins and the tail in Fig. 9B) do not fit our results as plotted. However, since we asked the computer to align the molecules by the best fit of the denatured areas without considering where the origin of replication would be located and since we were dealing with a small molecule with few denatured sites, we feel that these results are quite good. If the 8 molecules that do not fit were rotated 180° about the major denaturation area located in the left half of the molecules, 5 more molecules (asterisk, Fig. 9B) would have an origin coinciding with that of the other 31 molecules.

A comparison with the genetic map (Fig. 10) shows that this origin of ssDNA synthesis is between gene IV and gene II of the phage and that replication proceeds in a counterclockwise direction. Because both DNA and RNA chains grow in the 5′ → 3′ direction and because both M13 mRNA and progeny ssDNA syntheses occur on the complementary strand, one would expect the direction of DNA synthesis to be counterclockwise, as is RNA synthesis (21).

DISCUSSION

The precise mechanism of synthesis of progeny M13 RF and ssDNA is not yet completely

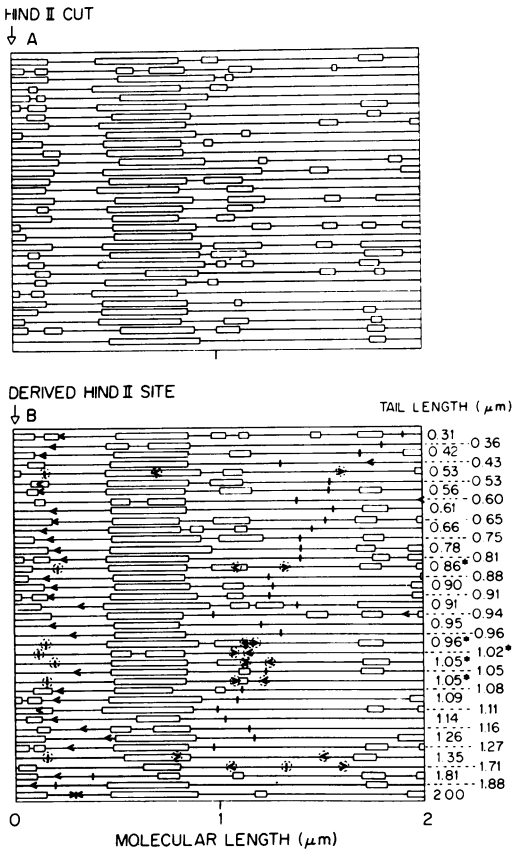

FIG. 9. *Denaturation maps of M13 RF molecules and σ structures. (A) M13 RFI DNA isolated from the heavy band described in Fig. 1 was cut with Hind endonuclease and partially denatured for electron microscopy as described in the text. The molecules, indicated by horizontal lines (the denatured regions are shown by open blocks), are aligned so that the major asymmetrically located, denatured region is in the left half of the molecules. (B) Circular RF molecules with tails (σ structures), present in the total phage DNA isolated from E. coli K37, 45 min after infection with wild-type M13 and partially denatured as described in the text, were aligned by computer for the best fit of the denatured areas, and transposed by computer to fit the profile of the Hind-cut molecules. The location and direction of the arrows indicate the origin and direction of replication, whereas the small vertical lines indicate the position of the tail. Molecules that have both origins and tails circled do not have an origin that fits our conclusion. The asterisk indicates molecules whose origins would fit if the molecules were rotated 180° about the major denatured area.*

understood. The lack of requirement for host *dna* functions other than that of *dnaE* (DNA polymerase III) in parental RF DNA synthesis (27), the requirement for several *dna* functions in progeny RF DNA synthesis (26), and the lack of requirement for many of the *dna* functions in progeny ssDNA synthesis (4, 20, 26) suggest that different replication complexes are responsible for the three different stages of intracellular M13 DNA replication. ϕX174, which also contains circular ssDNA as the genome, produces intermediates in DNA replication that are analogous to those of M13 (26). Dressler (6) showed that progeny ssDNA in ϕX174 is synthesized via the σ intermediate by displacement of the 5′ end of the viral strand in RF with a newly synthesized 3′ end of the same strand. Since then, Schröder and Kaerner (28) have shown that progeny RF DNA synthesis occurs by replication of the displaced single strand in the σ intermediates. It is obvious that progeny ssDNA is synthesized most economically by a strand displacement mechanism, i.e., one involving a σ structure. On the other hand, RF DNA could be synthesized in the same way or via a circular replicating intermediate, such as the structure observed in other systems (3, 14). Although this manuscript deals with the origin of ssDNA synthesis, our negative findings bring out some interesting possibilities regarding RF synthesis, which we will discuss first. Evidence based on studies with wild-type phage has been used to

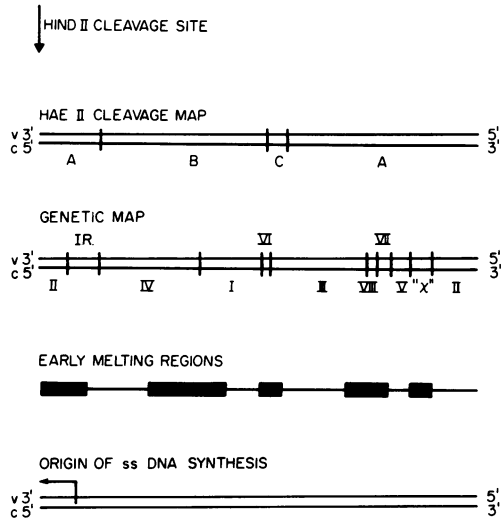

FIG. 10. *Origin of ssDNA synthesis on M13 phage genetic map. The HaeII restriction endonuclease cleavage map of RF DNA was used to compare the genetic map and the partial denaturation map as described in the text. The origin and direction of ssDNA synthesis indicated by the arrow was obtained from Fig. 9. (v) and (c) correspond to the virus and the complementary strand, respectively. The genetic map and HaeII restriction map are redrawn from reference 35.*

indicate that RF replication in M13 also occurs by a σ intermediate (29, 33), but our data do not support this model. We followed progeny RF DNA synthesis in the absence of progeny ssDNA synthesis by infecting suppressor-free *E. coli* K38 with M13 *am*5, in which RF replication continues for at least 50 min at 34°C in the complete absence of progeny ssDNA synthesis (S. Dasgupta and S. Mitra, unpublished data). Under these circumstances, we found no σ structures of RF among several hundred DNA molecules scored by electron microscopy and no pulse-labeled, longer-than-unit-length viral ssDNA after band sedimentation in alkaline sucrose (Fig. 5C). These findings suggest that M13 RF is not replicated in the same way as progeny ssDNA. Furthermore, the presence of DNA from both strands of RF DNA in both unit-length linear and smaller-than-unit-length fragments in nascent RF DNA after infection with *am*5 phage (Dasgupta and Mitra, unpublished data) supports a model of discontinuous synthesis of both strands in RF synthesis. In fact, we did see a few Cairns-type θ structures, which may be replicating intermediates of RF DNA. Their paucity in the DNA population could result from the fact that the replication time for RF is expected to be in the order of seconds, if the rate of DNA chain growth in RF is comparable to that in the host. Hence, it is quite possible that most of the molecules complete a round of replication even within the time the poison (used to stop the pulse label) inhibits DNA synthesis. Alternatively, the replicating RF molecules may be selectively lost either by binding very tightly to the membranous complex (29) or by existing in a structure that cannot be spread properly for electron microscopic visualization. Finally, the lack of σ structures with double-stranded tails after infection with wild-type phage makes it unlikely that the σ structure is involved in M13 RF replication in the manner postulated for φX174 (28).

On the other hand, our ultracentrifugal analyses of pulse-labeled M13 DNA confirm the σ mode of progeny ssDNA synthesis suggested by Ray (25). His experiments and those of Tseng and Marvin (33) indicated the presence of longer-than-unit-length, pulse-labeled strands in the virus strand of RF DNA after infection with wild-type phage. We showed by ultracentrifugal and enzymatic techniques that both longer-than-unit-length and unit-length DNA derived from pulse-labeled RFII DNA are of the viral-strand type and are indeed linear by the criterion of their susceptibility to exonuclease I. Furthermore, after a chase, the label can be transferred into circular DNA. These results, in agreement with the rolling-circle model of M13 ssDNA synthesis, are further supported by electron microscopic studies. Many σ structures with single-stranded tails covalently attached to RF molecules were readily observed in the electron microscope and constituted a significant proportion of the total intracellular RF pool. The occasional presence of RF molecules with two single-stranded tails was puzzling at first, but could easily be explained by incomplete branch migration in vitro (17). That the two tails are always attached to the RF in close proximity and that there is always a single-stranded region on the RF molecules between these points of attachment support such a possibility. It is obvious that branch migration is prevented in vivo, where the displaced single strand of σ structures is covered by gene 5 protein (24).

We have also observed several interesting aspects of the control of ssDNA synthesis. The σ model postulates a continuous elongation of the tail with a 5′ end via displacement by the growing 3′ end of the virus strand on the complementary strand template (10). After one round of replication, the single-stranded tail is cleaved and circularized into mature progeny ssDNA. We have first of all shown here that the tail in the σ structures is never longer than unit length, which indicates an efficient cleavage reaction independent of the DNA chain growth. Secondly, the fraction of RF DNA participating in ssDNA synthesis as rolling circles does not change significantly from early posinfection, when a very small amount of progeny ssDNA is detected, to late postinfection, when progeny ssDNA constitutes the bulk of the phage DNA synthesized. The amount of gene 5 protein also increases significantly late postinfection (26); therefore, our data suggest that gene 5 protein stimulates the synthesis of viral DNA via σ structures and thus controls such synthesis in a positive manner originally postulated by Staudenbauer and Hofschneider (30). Mazur and Model (19) showed that gene 5 protein controls M13 ssDNA synthesis in a negative fashion by preventing the ssDNA, complexed with gene 5 protein, from acting as a template for RF synthesis.

We have established that the unique origin of M13 ssDNA synthesis is located about 8% from the *Hin*d cleavage site, which corresponds to a location in *Hpa*II fragment F (34) and *Hae*III fragment G (12), and that the direction of its replication is counterclockwise on the conventional genetic map. Tabak et al. (32) have already established that the origin of parental RF DNA synthesis in vitro is also located in *Hpa*II fragment F; this region is the location of the intragenic space between genes IV and II (12).

During the preparation of this manuscript, the establishment of the origin of ssDNA synthesis in M13 phage was reported by two laboratories that relied upon the gradient of pulsed label in different regions of RF during ssDNA synthesis (12, 31). Our results agree remarkably well with these reports, although our investigation was entirely different in approach, being based on physical mapping of the origin and relying on the σ structure. The agreement therefore provides positive evidence for the involvement of σ structures as intermediates in ssDNA synthesis.

ACKNOWLEDGMENTS

This research was supported by the Energy Research and Development Administration under contract with the Union Carbide Corporation. A. T. Ganesan was supported by Public Health Service grant GM 108 and Research Career Development Award 6M 50199 from the National Institute of General Medical Sciences.

We thank Letha Oggs for her competent technical assistance and R. diLauro for the gift of *Hae*II restriction endonuclease.

LITERATURE CITED

1. **Bauer, W., and J. Vinograd.** 1971. The use of intercalative dyes in the study of closed circular DNA. Prog. Subcell. Mol. Biol. **2**:181-215.
2. **Blakesley, R. W., and R. D. Wells.** 1975. Single-stranded DNA from ϕX174 and M13 is cleaved by certain restriction endonucleases. Nature (London) **257**:421-422.
3. **Cairns, J.** 1963. The chromosome of *Escherichia coli*. Cold Spring Harbor Symp. Quant. Biol. **28**:43-46.
4. **Dasgupta, S., and S. Mitra.** 1976. The role of *Escherichia coli dnaG* function in coliphage M13 DNA synthesis. Eur. J. Biochem. **67**:47-51.
5. **Davis, R. W., and N. Davidson.** 1968. Electron microscope visualization of deletion mutations. Proc. Natl. Acad. Sci. U.S.A. **60**:243-250.
6. **Dressler, D.** 1970. The rolling circle for ϕX174 replication. II. Synthesis of single-stranded circles. Proc. Natl. Acad. Sci. U.S.A. **67**:1934-1942.
7. **Forsheit, A. P., D. S. Ray, and L. Lica.** 1971. Replication of bacteriophage M13. V. Single-strand synthesis during M13 infection. J. Mol. Biol. **57**:117-127.
8. **Fujimura, R. K., and E. Volkin.** 1968. Biochemical analysis of the naturally repaired sections of bacteriophage T5 deoxyribonucleic acid. I. Bromodeoxyuridine incorporation into parental deoxyribonucleic acid in the absence of deoxyribonucleic acid replication. Biochemistry **7**:3488-3498.
9. **Gefter, M. L.** 1975. DNA replication. Annu. Rev. Biochem. **44**:45-78.
10. **Gilbert, W., and D. Dressler.** 1968. DNA replications: the rolling circle model. Cold Spring Harbor Symp. Quant. Biol. **33**:473-484.
11. **Godson, G. N.** 1973. A simple method of preparing large amounts of ϕX RFI supercoiled DNA. Biochim. Biophys. Acta **299**:516-520.
12. **Horiuchi, K., and N. D. Zinder.** 1976. Origin and direction of synthesis of bacteriophage F1 DNA. Proc. Natl. Acad. Sci. U.S.A. **73**:2341-2345.
13. **Inman, R. B., and M. Schnös.** 1970. Partial denaturation of thymine and 5-bromouracil-containing λ DNA in alkali. J. Mol. Biol. **49**:93-98.
14. **Inselburg, J., and M. Fuke.** 1971. Isolation of catenated and replicating DNA molecules of colicin factor E1 from minicells. Proc. Natl. Acad. Sci. U.S.A. **68**:2839-2842.
15. **Jacobson, M. K., and K. G. Lark.** 1973. DNA replication in *Escherichia coli*: evidence for two classes of small deoxyribonucleotide chains. J. Mol. Biol. **73**:371-396.
16. **Kleinschmidt, A. K., D. Lang, D. Jacherts, and R. K. Zahn.** 1962. Preparation and length measurements of the total deoxyribonucleic acid content of T2 bacteriophage. Biochim. Biophys. Acta **61**:857-864.
17. **Lee, C. S., R. W. Davis, and N. Davidson.** 1970. A physical study by electron microscopy of the terminally repetitious, circularly permuted DNA from the coliphage particles of *Escherichia coli* 15. J. Mol. Biol. **48**:1-22.
18. **Lyons, L. B., and N. D. Zinder.** 1972. The genetic map of the filamentous bacteriophage F1. Virology **49**:45-60.
19. **Mazur, B. J., and P. Model.** 1976. Regulation of coliphage F1 single-stranded DNA synthesis by a DNA-binding protein. J. Mol. Biol. **78**:285-300.
20. **Mitra, S., and D.R. Stallions.** 1976. The role of *Escherichia coli dnaA* gene and its integrative suppression in M13 coliphage DNA synthesis. Eur. J. Biochem. **67**:37-45.
21. **Model, P., and N. D. Zinder.** 1974. In vitro synthesis of bacteriophage F1 proteins. J. Mol. Biol. **83**:231-251.
22. **Okazaki, R.** 1974. Short chain intermediates in DNA replication, p. 1-32. *In* R. B. Wickner (ed.), Methods in molecular biology, vol. 7. Marcel Dekker, Inc., New York.
23. **Pratt, D., and W. S. Erdahl.** 1968. Genetic control of bacteriophage M13 DNA synthesis. J. Mol. Biol. **37**:181-200.
24. **Pratt, D., P. Laws, and J. Griffith.** 1974. Complex of bacteriophage M13 single-stranded DNA and gene 5 protein. J. Mol. Biol. **82**:425-439.
25. **Ray, D. S.** 1969. Replication of bacteriophage M13. II. The role of replicative forms in single-strand synthesis. J. Mol. Biol. **43**:631-643.
26. **Ray, D. S.** 1977. Replication of filamentous bacteriophages, p. 105-178. *In* H. Fraenkel-Conrat and R. R. Wagner (ed.), Comprehensive virology, vol. 7. Plenum Publishing Corp., New York.
27. **Schekman, R., A. Weiner, and A. Kornberg.** 1974. Multienzyme systems of DNA replication. Science **186**:987-993.
28. **Schröder, C. H., and H. C. Kaerner.** 1972. Replication of bacteriophage ϕX174 replicative form DNA *in vivo*. J. Mol. Biol. **71**:351-362.
29. **Staudenbauer, W. L., and P. H. Hofschneider.** 1971. Membrane attachment of replicating parental DNA molecules of bacteriophage M13. Biochem. Biophys. Res. Commun. **42**:1035-1041.
30. **Staudenbauer, W. L., and P. H. Hofschneider.** 1973. Replication of bacteriophage M13: positive role of gene 5 protein in single-stranded DNA synthesis. Eur. J. Biochem. **34**:569-576.
31. **Suggs, S. V., and D. S. Ray.** 1977. Replication of bacteriophage M13. XI. Localization of the origin for M13 single-strand synthesis. J. Mol. Biol. **110**:147-163.
32. **Tabak, H. F., J. Griffith, K. Geider, H. Schaller, and A. Kornberg.** 1974. Initiation of deoxyribonucleic acid synthesis. VII. A unique location of the gaps in M13 replicative duplex synthesized *in vitro*. J. Biol. Chem. **249**:3049-3054.
33. **Tseng, B. Y., and D. A. Marvin.** 1972. Filamentous bacterial viruses. V. Asymmetric replication of fd duplex deoxyribonucleic acid. J. Virol. **10**:371-383.
34. **van den Hondel, C. A., and J. G. G. Schoenmakers.** 1975. Studies on bacteriophage M13 DNA. I. A cleavage map of the M13 genome. Eur. J. Biochem. **53**:547-558.
35. **van den Hondel, C. A., and J. G. Schoenmakers.** 1976. Cleavage maps of the filamentous bacteriophages M13, fd, f1 and ZJ/2. J. Virol. **18**:1024-1039.
36. **Young, I. T., D. Levinstone, M. Eden, B.-K. Tye, and D. Botstein.** 1974. Alignment of partial denaturation maps of circularly permuted DNA by computer. J. Mol. Biol. **85**:528-532. (Appendix in J. Mol. Biol. **85**:501-532, 1974.)